Cellular regulation of extension and retraction of pseudopod-like blebs produced by nanosecond pulsed electric field (nsPEF)

Mikhail A. Rassokhin[*] and **Andrei G. Pakhomov**

Abstract

Recently we described a new phenomenon of anodotropic pseudopod-like blebbing in U937 cells exposed to nanosecond pulsed electric field (nsPEF). In Ca^{2+}-free buffer such exposure initiates formation of pseudopod-like blebs (PLBs), protrusive cylindrical cell extensions that are distinct from apoptotic and necrotic blebs. PLBs nucleate predominantly on anode-facing cell pole and extend towards anode during nsPEF exposure. Bleb extension depends on actin polymerization and availability of actin monomers. Inhibition of intracellular Ca^{2+}, cell contractility and RhoA produced no effect on PLB initiation. Meanwhile, inhibition of WASP by wiskostatin causes dose-dependent suppression of PLB growth. Soon after the end of nsPEF exposure PLBs lose directionality of growth and then retract. Microtubule toxins nocodazole and paclitaxel did not show immediate effect on PLBs; however, nocodazole increased mobility of intracellular components during PLB extension and retraction. Retraction of PLBs is produced by myosin activation and corresponding increase in PLB cortex contractility. Inhibition of myosin by blebbistatin reduces retraction while inhibition of RhoA-ROCK pathway by Y-27632 completely prevents retraction. Contraction of PLBs can produce cell translocation resembling active cell movement. Overall, the formation, properties, and lifecycle of PLBs share common features with protrusions associated with amoeboid cell migration. PLB lifecycle may be controlled through activation of WASP by its upstream effectors such as Cdc42 and PIP2, and main ROCK activator - RhoA. Parallels between pseudopod-like blebbing and motility blebbing may provide new insights into their underlying mechanisms.

Keywords

Electroporation; Nanosecond pulsed electric field; Blebbing; Actin polymerization; Membrane protrusion; Cell cortex; Cell motility

Introduction

Pulsed electric fields induce permeabilization of plasma membrane that leads to water uptake and transmembrane ion transport (Schoenbach et al. 2007). Water uptake follows Donnan-type colloid osmotic mechanism and manifests in cell swelling (Tsong 1991) and blebbing (Gass and Chernomordik 1990). Blebbing of the cell membrane occurs predominantly in the areas of weak membrane to cytoskeleton adhesion (Cunningham 1995)

[*]Corresponding author. Frank Reidy Research Center for Bioelectrics, Old Dominion University, 4211 Monarch Way Ste 300, Norfolk, VA, USA 23508, Tel.: +1-757-337-9748, Fax: +1-757-451-1010, mrass002@odu.edu.

and cell cortex breakage (Paluch et al. 2005). Alternatively, blebbing may result from the increase in cortex contractility (Mills et al. 1998) and associated rise in the intracellular pressure (Charras 2008). The exact mechanisms of blebbing in cells exposed to pulsed electric fields (PEF) are not yet known. Typical PEF-induced blebs are clear non-retractable spherical membrane extensions that develop during or after pulse exposure (Tekle et al. 2008). Nanosecond pulsed electric field (nsPEF) exposure also produces blebbing (Pakhomov et al. 2007). Morphologically these blebs are similar to blebs described for other types of stress (Barros et al. 2003). Recently we reported a new nsPEF-induced type of blebbing that shows features characteristic for physiological rather than stress-induced blebbing (Rassokhin and Pakhomov 2012). Pseudopod-like blebs (PLBs) that form in U937 cells in Ca^{2+}-free conditions exhibit directional growth during nsPEF treatment. Moreover, PLBs are polarized and retractable membrane protrusions similar to blebs of migrating cells (Fackler and Grosse 2008; Charras and Paluch 2008). The knowledge collected about blebbing motility to date (Yoshida and Soldati 2006) may allow ones to infer the mechanisms of electroporation-induced PLBs.

Cells migrate through repetitive cycles of membrane extension and retraction (Pollard and Borisy 2003), and rely on two distinct modes of translocation - mesenchymal and amoeboid motility, distinguished by protrusion morphology and regulation (Bergert et al. 2012). Mesenchymal cells predominantly develop actin-rich protrusions, lamellipodia and filopodia on the leading edge, and contractile actomyosin filaments on the trailing edge (Etienne-Manneville and Hall 2002). Amoeboid cells employ bleb-like protrusions driven by intracellular pressure rather than by actin polymerization (Petrie et al. 2012). While actin-based mesenchymal migration relies on specific adhesion interactions (e.g., integrins) with extracellular matrix (ECM) (Wolf et al. 2003a), amoeboid migration allows cells to squeeze through ECM autonomously (Lammermann et al. 2008) employing just low-affinity non-specific interactions with matrix barriers (Renkawitz and Sixt 2010). Low substrate dependence and reliance on contraction-driven propulsion makes blebbing motility an effective strategy for cancer invasion (Parri et al. 2009) and extravascular leukocyte migration (Wolf et al. 2003b). Migration velocity through amoeboid translocation may reach 20 μm/min in contrast to mesenchymal migration velocity of 1 μm/min (Friedl and Wolf 2003b). Blebbing motility follows basic migration steps - reversible membrane detachment on the front end, forward cytoplasm streaming and contraction of the cell rear end (Blaser et al. 2006). Regulators of blebbing motility at different stages of bleb cycle may be important for identification of regulators of nsPEF-induced PLBs.

While formation of actin-rich protrusions is studied at length, molecular mechanisms of blebbing only begins to emerge (Ridley 2011). Regulation of actin protrusion assembly by Rho family of small GTPases, namely by the best studied members Cdc42, Rac1 and RhoA, is a widely accepted notion (Raftopoulou and Hall 2004). Cdc42 and Rac1 promote actin polymerization and formation of actin-rich protrusions (Ridley et al. 1992; Keely et al. 1997), while RhoA regulates assembly of actomyosin responsible for trailing edge retraction and contractility of the cell cortex (Salbreux et al. 2012). Although the role of small GTPases in blebbing motility is deemed important, the detailed effects on different bleb stages are not yet clear (Ridley 2011). Cdc42 regulates cell polarization (Etienne-Manneville 2004; Yam et al. 2007) and maintenance of amoeboid and mesenchymal cell morphology

(Lämmermann et al. 2009; Gadea et al. 2008). The role of Rac1 and RhoA is less clear. Some reports suggest that both GTPases take part in bleb extension (Kardash et al. 2010), while others state that Rac1 and RhoA play distinct and mutually exclusive roles in amoeboid and mesenchymal migration (Sanz-Moreno et al. 2008). The antagonism between Rac1 and RhoA is well established (Rottner et al. 1999) and may act as a regulatory switch between actin- and bleb-driven migration modes (Parri and Chiarugi 2010). Cells with high Rac1 activity generally favor actin-driven mesenchymal migration (Sanz-Moreno 2012) in agreement with central role of Rac1 in actin protrusion formation (Steffen et al. 2004). Meanwhile, cells with high RhoA activity exhibit bleb-driven amoeboid migration (Sahai and Marshall 2003) consistently with the modulatory role of this GTPase in actomyosin contractility. Contractility may cause fluctuation in internal cell pressure, thereby causing disruption of membrane-cytoskeleton adhesion and bleb nucleation (Maugis et al. 2010). In non-muscle cells RhoA regulates actomyosin contractility through its main effector Rho kinase (ROCK) (Leung et al. 1996). ROCK activates non-muscle myosin II (NM II) through phosphorylation of myosin regulatory light chain (MLC) (Vicente-Manzanares et al. 2009) and inhibition of myosin light chain phosphatase (MLCP), an enzyme removing activating phosphate from MLC (Kimura et al. 1996). Presumably, ROCK is also able to activate MLC directly (Amano et al. 1996). Another potent modulator of NM II is myosin light chain kinase (MLCK) (Tan et al. 1992). MLCK is activated by Ca^{2+}-calmodulin and, unlike ROCK, exerts its stimulatory effect on MLC in response to changes in Ca^{2+} concentration (Paul et al. 1999; Fukata et al. 2001). The role of small GTPases in cell motility and blebbing makes them central candidates for regulation of protrusive activity in PLBs.

Actin polymerization and actomyosin contractility play a central role in protrusion and bleb formation; however their implication in pseudopod-like blebbing is not yet clear. PLBs represent a polarized and directed cell response that is likely coordinated by the same mechanisms as other cell protrusions. Identification of factors responsible for conversion of nsPEF stimulus into membrane and cytoskeleton rearrangements is central for understanding of pulse-induced effects on cells. Investigation of these mechanisms may help to produce a model for studying of blebbing motility. Such motility is shown to be important in cancer dissemination (Friedl and Wolf 2003a), leukocyte and primordial germ cells migration (Takesono et al. 2010). Here, we investigate the mechanisms of nsPEF-induced PLBs and discuss their relevance to blebbing motility.

Materials and Methods

Cell Line and Propagation

U937 human promonocytic cell line was obtained from the ATCC (Mannanas, VA) and propagated at 37 °C with 5 % CO_2 in air. Cells were grown in RPMI 1640 medium containing Lglutamine and supplemented with 10 % fetal bovine serum and 1% penicillin/streptomycin. Cell culture components were obtained from Atlanta Biologicals (Norcross, GA) or Mediatech Cellgro (Herndon, VA).

Fluorescent dyes, experimental buffers and chemicals

All experiments were performed in a bath buffer that contained (in mM) 135 NaCl, 5 KCl, 4 MgCl$_2$, 10 HEPES, 2 Na-EGTA and 10 glucose at pH 7.4 and osmolality of about 290 mOsm/kg. Oregon Green® 488-phalloidin and BAPTA-AM were purchased from Invitrogen (Eugene, OR). Wiskostatin was purchased from Tocris Bioscience (Bristol, United Kingdom). Jasplakinolide was obtained from Santa Cruz Biotechnology (Santa Cruz, CA) and exoenzyme C3 transferase (RhoA inhibitor) from Cytoskeleton (Denver, CO). Other chemicals, including thapsigargin, (−)-blebbistatin, latrunculin A, nocodazole, paclitaxel and Y-27632 were purchased from Sigma–Aldrich (St. Louis, MO). Oregon Green® 488-phalloidin was dissolved in 100 % methanol to obtain 6.6 μM stock solution which was added to a final concentration of 13.3 nM to the experimental buffer. All other reagents were dissolved in 100 % DMSO. In experiments where vehicle-to-buffer concentration exceeded 1:1000 ratio, vehicle was used as a negative control, 0.1% DMSO in blebbistatin series and 0.25% DMSO in Y-27632 series. In experiments using 13 μM BAPTA-AM and 50 nM thapsigargin, cells were preincubated at room temperature with reagents in the bath buffer for 30 or 15 min, respectively. In blebbistatin series, cells were preincubated with 100 μM blebbistatin at 37°C for 30 min in the full growth medium. The exposure of cells to reagents in the microscope chamber before pulse delivery and data recording was kept to a minimum and typically did not exceed 3 min.

Cell Imaging and Image Analysis

For live cell time lapse imaging, a suspension of U937 cells was transferred into a Petri dish with fibronectin-covered glass coverslips (Neuvitro Corporation, El Monte, CA). The suspension was left in incubator for at least 30 min to allow cells to precipitate onto the coverslip surface. Then the coverslip was briefly washed in the bath buffer and transferred to the microscope. Image recording was performed in a glass-bottomed chamber (Warner Instruments, Hamden, CT) mounted on an IX81motorized inverted microscope (Olympus, Center Valley, PA). Differential-interference contrast (DIC) and fluorescence imaging were performed using a 40× dry objective with (NA 0.95). Cell images were recorded using a FV1000 confocal laser scanning system (Olympus). Typically images were taken at regular intervals of 2–5 s. Recordings started concurrently with a 2-min nsPEF treatment and continued for 5–8 min after the end of pulse exposure.

All experiments were performed at a room temperature of 22–24 °C. Cell images were quantified using FluoView v. 3.1 (Olympus) and MetaMorph v. 7.7 (Molecular Devices, Sunnyvale, CA) software.

nsPEF treatment and Local Electric Field Modeling

Exposure of individual cells to nsPEF was performed as described previously (Bowman et al. 2010). Pulses were delivered to a group of 3–6 cells with a pair of custom tungsten rod electrodes (0.08 mm diameter, 0.15 mm gap). Electrodes were positioned at 50 μm above the coverslip surface using a robotic micromanipulator (MP-225; Sutter, Novato, CA), so that the selected cells were located in the center between their tips (Fig. 1). Nearly rectangular 60-ns pulses were generated in a transmission line-type circuit, by closing a MOSFET switch upon a timed delivery of a TTL trigger pulse from pClamp software via a

Digidata 1322A output (MDS, Foster City, CA). The exact nsPEF delivery protocol and synchronization of nsPEF delivery with image acquisition were programmed in pClamp. In all experiments described in this paper, cells were exposed to 2400 pulses at 12 kV/cm; the pulse repetition rate was 20 Hz, so the entire treatment lasted 120 s. These optimal pulse conditions were established previously (Rassokhin and Pakhomov 2012). The E-field between the electrodes was determined by a 3D simulation with a finite element Maxwell equation solver Amaze 3D (Field Precision, Albuquerque, NM). Exact nsPEF shapes and amplitudes were captured and measured with a Tektronix TDS 3052 oscilloscope (Beaverton, OR). Experiments included appropriate controls in which cells were subjected to identical manipulations but without tested substances.

Results

Lifecycle of pseudopod-like blebs

Pseudopod-like blebbing was studied on U937 cells exposed to long trains of nsPEF. In a typical experiment a group of cells loosely attached to the coverslip was positioned between two pulse-delivering electrodes (Fig. 1) and exposed to nsPEF as described above.

PLB lifecycle can be divided into separate consecutive stages (Fig. 2). Initially, bleb formation starts with nucleation predominantly on anode-facing cell surface after 15–30 seconds of pulse treatment. Before nucleation the cell may exhibit minor rounding and smoothing of surface features. After nucleation, the bleb begins a steady and gradual extension towards the anode under continual nsPEF exposure. Upon advancement, the leading edge of PLB leaves behind a translucent longitudinal stalk. Although the stalk may bend and leave the focal plane, the growth direction is almost exclusively anodotropic and is maintained throughout the whole exposure duration. Even PLBs that nucleate on cell flanks commonly deflect towards anode early in the extension (Fig. 3A). Typical PLB extends from the cell surface for as much as 30 μm. When exposure stops, the bleb growth may continue for a period of 15–60 s; however, without nsPEF the growth direction becomes random (Fig. 3B).

After the end of pulse treatment and a short period of stabilization PLBs start to retract. Retraction results in a partial reduction in bleb length and width. The extent of retraction varies drastically among cells, from barely detectable crumpling to almost complete pulling back into the cell body. During the retraction, PLBs assume crumpled contracted appearance concurrently with swelling of the cell body and/or *de novo* formation of secondary rounded blebs (Fig. 3C). The elevated position of pulse-delivering electrodes favors the extension of PLBs into the solution. However, even in such configuration PLB growth tip can make contact with the coverslip surface. In this case, PLB gets attached to the coverslip and its retraction pulls the cell body forward causing cell translocation (Fig. 3D).

Fluorescent actin labeling

Development of membrane pores due to pulse treatment renders cell membrane permeable to small organic compounds including fluorescent molecules such as Oregon green® 488-phalloidin conjugate (MW ~ 1180). The uptake of fluorescent phalloidin conjugates results

in fast labeling of cellular actin (Rassokhin and Pakhomov 2012). Such uptake starts immediately after the beginning of nsPEF application and by the moment of PLB nucleation, the actin staining develops to the full extent. Actin labeled with Oregon green® 488-phalloidin is initially confined to cell soma, but as PLB grows the conjugate stains bleb cortex (Fig. 4). Bleb interior remains largely devoid of actin; however, the base region of PLB commonly shows a portion of actin-rich cell components protruding into bleb lumen through the bleb neck. Bleb cortex remains seemingly steady during the bleb growth but in retraction bleb assumes crumpled appearance that is manifested in further fluorescent staining development corresponding to increased cortex thickness. Retracting bleb gradually shortens, and its folded membrane takes up most of the bleb interior that in turn produces intense actin fluorescence. In the most explicit scenario PLB may retract completely or leave behind only a small actin-rich spike.

The role of contractility in PLB extension and retraction

Bleb studies suggest that cortex contractility is essential for stimulation of blebbing (Paluch et al. 2006). Cell contractility in nsPEF treated cells may be stimulated by intracellular calcium increase. Even though PLB experiments are performed in a Ca^{2+}-free buffer, nsPEF exposure stimulates the release of intracellular Ca^{2+} that may rise to physiologically relevant concentrations (White et al. 2004; Semenov et al. 2012). In order to establish the implications of intracellular Ca^{2+} release on PLB initiation we incubated cells in a Ca^{2+}-free buffer with Ca^{2+} chelator BAPTA-AM or reticulum Ca^{2+}-ATPase inhibitor thapsigargin. After incubation U937 cells were still able to produce PLBs (not shown). These results suggest that intracellular Ca^{2+} release does not play an essential role in PLB development. Cell cortex contractility can also be suppressed by a myosin inhibitor blebbistatin and RhoA-ROCK inhibitor Y-27632 (Paluch et al. 2005). Inhibition of the cortex contractility by a myosin ATPase inhibitor blebbistatin (Kovács et al. 2004) is attained through specific inhibition of non-muscle myosin isoforms (Limouze et al. 2004). Our experiments established that PLB-forming capacity of U937 cells is not affected by blebbistatin. The average bleb lengths in control and treatment groups were not significantly different. At the same time, bleb retraction was significantly inhibited, although the inhibition was only partial even at the maximal tested drug concentration (Fig. 5). Likewise, cell treatment with a RhoA-ROCK inhibitor Y-27632 did not prevent PLBs extension but could fully block their retraction and crumpling leaving PLBs completely static (Fig. 5). PLBs formed in the presence of Y-27632 were slightly but significantly shorter than PLBs in controls. A specific RhoA inhibitor C3 transferase (Vega et al. 2011), also did not prevent PLB formation (not shown) suggesting that RhoA does not play an essential role in PLB extension but is necessary for its retraction.

Actin filament but not microtubule toxins inhibit PLB formation

Toxins affecting actin polymerization prevent formation of PLBs. Actin polymerization inhibitor latrunculin A (Coué et al. 1987) at the concentration of 100 nM causes almost complete inhibition of PLB growth and this inhibition is not caused by the interference with bleb nucleation (Fig. 6). According to the poroelastic cell model actin inhibition may suppress bleb nucleation due to degradation of cell cortex (Mitchison et al. 2008). With regard to PLBs such degradation could prevent initiation of their formation. However,

despite significant inhibition of PLB extension, latrunculin A did not prevent bleb nucleation *per se*. Inhibition of nucleation by 100 nM latrunculin A started after at least 10-min incubation. In that case, nsPEF treatment produced uniform cell swelling but no blebs (not shown). Another actin toxin, jasplakinolide, also demonstrated PLB inhibition. Jasplakinolid increases the rate of actin nucleation and stabilizes F-actin leading to depletion of actin pool (Bubb et al. 1994). Cells exposed to pulses immediately after being placed in the buffer with 1 μM jasplakinolide were able to form and retract PLBs. However, cell exposure after 10-min incubation with 1 μM jasplakinolide resulted in a random nucleation of non-retractable spherical blebs on the cell surface (not shown).

We also investigated the effect of tubulin toxins nocodazole and paclitaxel on PLB formation. Pulse exposure of cells in the presence of 1 μM or 10 μM of nocodazole, a microtubule inhibitor (Ganguly et al. 2012), did not prevent PLB development. Interestingly, due to nocodazole, nuclei of some cells completely protracted from the cell body into PLB interior during its retraction phase (Fig. 7). Incubation of U937 cells with 10 μM nocodazole for 10 min caused their disfiguration and such cells did not produce PLBs. Paclitaxel, a tubulin stabilizing reagent (Jordan et al. 1993), at 1 and 10 μM did not seemingly affect PLB extension or retraction with or without 10 min incubation (data not shown).

PLB growth is suppressed by inhibition of Wiskott-Aldrich syndrome protein

Actin polymerization is essential for PLB formation; however, upstream effectors of polymerization are not clear. RhoA inhibition and contractility suppression do not affect PLB extension stage. We tested whether bleb extension is affected by wiskostatin, the inhibitor of Wiskott-Aldrich syndrome protein (WASP) activation that also prevents WASP interaction with upstream effectors such as Cdc42 and PIP2 (Deacon and Peterson 2008). WASP activation is essential for activation of actin polymerization (Rohatgi et al. 1999). WASP activates Apr2/3, a complex that stimulates actin nucleation and branching and thereby *de novo* formation of actin filaments (Campellone and Welch 2010). Wiskostatin can inhibit WASP interaction with Cdc42 (Peterson et al. 2004), a major cytoskeleton regulator in mesenchymal and amoeboid motility. Indeed, we found that wiskostatin caused a dose-dependent suppression of PLB growth (Fig. 8). PLBs formed in the presence of wiskostatin were wider and shorter than those in controls (Fig. 8, inset). While 2 μM wiskostatin had no effect on PLB growth, the presence of 10 μM wiskostatin significantly reduced the PLB length. In the highest tested wiskostatin concentration (25μM) nsPEF induced formation of short rounded blebs on the anodic cell pole.

Discussion

Pseudopod-like blebbing represents a coordinated response to permeabilization of the plasma membrane by nsPEF. Such response is not produced by a direct physical effect of pulses on cellular molecules (i.e. electrophoresis) but rather represents a cell reaction to water uptake through a Donnan-type colloid-osmotic mechanism (Rassokhin and Pakhomov 2012). PLB extension is guided by nsPEF presumably due to support of local permeabilized state of anodic cell pole. Electrical potential imposed on the cell membrane during pulse application favors permeabilization of anodic pole due to enhancement of induced

transmembrane potential by resting membrane potential. The connection between continual high-rate pulse application and permeabilization is highlighted by two observations: (1) after exposure termination, permeabilization may sustain and feed a sluggish bleb extension; however, pulse guiding effect is terminated which results in a random drift of growth direction, and (2) when PLBs are nucleated on cell flanks instead of the anodic pole, they maintain anodotropic growth direction, further suggesting that pulse stimulation provides guidance throughout the whole treatment.

PLB maintains elongated shape and growth through actin polymerization utilizing free actin pool. Oregon-Green® 488-phalloidin conjugate staining shows that actin is associated with PLB membrane from the beginning of bleb extension. Cell exposure to latrunculin A, an actin polymerization inhibitor, completely prevents PLB extension. Besides actin polymerization, latrunculin A may also disrupt cortical actin of cell soma (Hummel et al. 2011) that may prevent PLB nucleation. We demonstrated that latrunculin A inhibits PLBs before it prevents bleb nucleation, thereby cells lose ability to produce PLBs but form static rounded blebs. Disruption of the cell cortex and complete inhibition of bleb nucleation requires at least 10-min incubation with latrunculin A. Experiments with jasplakinolide prove that PLB growth also relies on free actin. Immediate cell exposure to 1 μM jasplakinolide does not affect PLB formation; however, after 10-min incubation the nsPEF treatment causes the formation of regular rounded blebs only. This effect is explained by depletion of cellular pool of free actin (Bubb et al. 2000), thus making actin monomers unavailable for PLB extension. Although the exposure to actin toxins and drug concentrations were kept at minimum, we cannot exclude the development of more complex cellular effects and alternative explanations to these data.

Microtubules seem not to play an immediate role in PLB lifecycle. Inhibition of microtubules by 1 μM nocodazole has no apparent effect on PLBs, while 10 μM nocodazole inhibits PLBs causing apparent cells disfiguration. Interestingly, nocodazole treatment facilitates translocation of nucleus into PLB. This effect may be interesting in view of reports about stimulating effect of tubulin toxins on blebbing motility (Eitaki et al. 2012). The lack of definitive role of microtubules in PLB formation was further supported by the absence of paclitaxel effect.

Small GTPases play an important role in protrusion formation and blebbing motility. Here, we show that contrary to blebbing motility, RhoA and cortex contractility are not essential for PLB nucleation and extension. Meanwhile, PLB retraction is driven by actomyosin contractility that requires activation via RhoA-ROCK dependent pathway. Such regulation is consistent with retraction mechanisms in physiological blebs (Charras et al. 2006). During retraction PLBs demonstrate slow shrinkage and crumpling. Due to contraction of PLB, the liquid extruded into cell body causes swelling and/or formation of secondary rounded blebs. The trigger for retraction is not yet clear; however, its activation apparently requires termination of permeabilizing nsPEF treatment and deactivation of PLB extension mechanisms.

PLB extension relies on actin polymerization due to WASP activation that may be caused by upstream effectors of WASP, such as Cdc42 or PIP2. Inhibition of WASP by wiskostatin

showed dose-dependent suppression of PLB extension. In the presence of wiskostatin PLBs are still nucleated on the anodic cell pole; however their length is significantly smaller. Short PLBs formed in the presence of wiskostatin maintain polarity and protrusive growth. Of note, effects of wiskostatin on PLBs develop at low concentrations and do not require incubation that reportedly causes toxicity in cells (Guerriero and Weisz 2007). Further confirmation of the role of WASP and ROCK effectors, such as small GTPases Cdc42 and RhoA, will require more specific approaches that are currently impeded by low efficiency of genetic manipulations in U937 cells (Martinet et al. 2003).

The above experiments clearly show that under Ca^{2+}-free conditions, nsPEF treatment can initiate and guide the formation of protrusive extensions, PLBs, in U937 cells. In the presence of Ca^{2+} in the experimental buffer (e.g., 2 mM) nsPEF treatment instead of PLBs produces diffuse blebbing succeeded by microvesiculation. These irreversible changes, particularly in hematologic cells like U937, are consistent with Ca^{2+}-induced toxicity and presumably cell death. In contrast to diffuse blebs PLB lifecycle is orchestrated by coordinated rearrangements of the cell cytoskeleton. PLB extension is maintained by the activation of actin polymerization, while retraction requires activation of myosin contractility. PLBs retraction can be coupled to the cell body translocation, and therefore may serve as a simple model of bleb motility. We provide evidence that PLB lifecycle may be controlled by WASP and ROCK effectors, such as Cdc42 and RhoA. Considering wide implications of these GTPases in cell physiology (Bustelo et al. 2007), their further investigation may provide new insights for the use of nsPEF technology in biomedical applications. PLBs may provide a valuable tool for investigation of bleb-like protrusions and their correspondence to actin-driven cellular protrusions (Lämmermann and Sixt 2009). Although physiological relevance of PLBs is yet to be determined, using nsPEF to induce cell polarization, directed membrane extension and cell locomotion offers prospects for further investigation.

Bibliography

Amano M, Ito M, Kimura K, Fukata Y, Chihara K, Nakano T, Matsuura Y, Kaibuchi K. Phosphorylation and Activation of Myosin by Rho-associated Kinase (Rho-kinase). Journal of Biological Chemistry. 1996; 271(34):20246–20249. [PubMed: 8702756]

Barros LF, Kanaseki T, Sabirov R, Morishima S, Castro J, Bittner CX, Maeno E, Ando-Akatsuka Y, Okada Y. Apoptotic and necrotic blebs in epithelial cells display similar neck diameters but different kinase dependency. Cell Death Differ. 2003; 10(6):687–697. [PubMed: 12761577]

Bergert M, Chandradoss SD, Desai RA, Paluch E. Cell mechanics control rapid transitions between blebs and lamellipodia during migration. Proceedings of the National Academy of Sciences. 2012; 109(36):14434–14439.

Blaser H, Reichman-Fried M, Castanon I, Dumstrei K, Marlow Florence L, Kawakami K, Solnica-Krezel L, Heisenberg C-P, Raz E. Migration of Zebrafish Primordial Germ Cells: A Role for Myosin Contraction and Cytoplasmic Flow. Developmental Cell. 2006; 11(5):613–627. [PubMed: 17084355]

Bowman A, Nesin O, Pakhomova O, Pakhomov A. Analysis of Plasma Membrane Integrity by Fluorescent Detection of Tl(+) Uptake. Journal of Membrane Biology. 2010; 236(1):15–26. [PubMed: 20623351]

Bubb MR, Senderowicz AM, Sausville EA, Duncan KL, Korn ED. Jasplakinolide, a cytotoxic natural product, induces actin polymerization and competitively inhibits the binding of phalloidin to F-actin. Journal of Biological Chemistry. 1994; 269(21):14869–14871. [PubMed: 8195116]

Bubb MR, Spector I, Beyer BB, Fosen KM. Effects of Jasplakinolide on the Kinetics of Actin Polymerization: An Explanation For Certain *in vivo* Observations. Journal of Biological Chemistry. 2000; 275(7):5163–5170. [PubMed: 10671562]

Bustelo XR, Sauzeau V, Berenjeno IM. GTP-binding proteins of the Rho/Rac family: regulation, effectors and functions in vivo. BioEssays. 2007; 29(4):356–370. [PubMed: 17373658]

Campellone KG, Welch MD. A nucleator arms race: cellular control of actin assembly. Nat Rev Mol Cell Biol. 2010; 11(4):237–251. [PubMed: 20237478]

Charras G, Paluch E. Blebs lead the way: how to migrate without lamellipodia. Nat Rev Mol Cell Biol. 2008; 9(9):730–736. [PubMed: 18628785]

Charras GT. A short history of blebbing. Journal of Microscopy. 2008; 231(3):466–478. [PubMed: 18755002]

Charras GT, Hu C-K, Coughlin M, Mitchison TJ. Reassembly of contractile actin cortex in cell blebs. The Journal of Cell Biology. 2006; 175(3):477–490. [PubMed: 17088428]

Coue M, Brenner SL, Spector I, Korn ED. Inhibition of actin polymerization by latrunculin A. FEBS Letters. 1987; 213(2):316–318. [PubMed: 3556584]

Cunningham CC. Actin polymerization and intracellular solvent flow in cell surface blebbing. The Journal of Cell Biology. 1995; 129(6):1589–1599. [PubMed: 7790356]

Deacon, SW.; Peterson, JR. Chemical Inhibition Through Conformational Stabilization of Rho GTPase Effectors. In: Klussmann, E.; Scott, J., editors. Protein-Protein Interactions as New Drug Targets, vol 186. Handbook of Experimental Pharmacology. Springer Berlin Heidelberg; 2008. p. 431-460.

Eitaki M, Yamamori T, Meike S, Yasui H, Inanami O. Vincristine enhances amoeboid-like motility via GEF-H1/RhoA/ROCK/Myosin light chain signaling in MKN45 cells. BMC Cancer. 2012; 12(1):469. [PubMed: 23057787]

Etienne-Manneville S. Cdc42 - the centre of polarity. Journal of Cell Science. 2004; 117(8):1291–1300. [PubMed: 15020669]

Etienne-Manneville S, Hall A. Rho GTPases in cell biology. Nature. 2002; 420(6916):629–635. [PubMed: 12478284]

Fackler OT, Grosse R. Cell motility through plasma membrane blebbing. The Journal of Cell Biology. 2008; 181(6):879–884. [PubMed: 18541702]

Friedl P, Weigelin B. Interstitial leukocyte migration and immune function. Nat Immunol. 2008; 9(9): 960–969. [PubMed: 18711433]

Friedl P, Wolf K. Proteolytic and non-proteolytic migration of tumour cells and leucocytes. Biochem Soc Symp. 2003a; (70):277–285. [PubMed: 14587300]

Friedl P, Wolf K. Tumour-cell invasion and migration: diversity and escape mechanisms. Nat Rev Cancer. 2003b; 3(5):362–374. [PubMed: 12724734]

Fukata Y, Kaibuchi K, Amano M. Rho–Rho-kinase pathway in smooth muscle contraction and cytoskeletal reorganization of non-muscle cells. Trends in Pharmacological Sciences. 2001; 22(1): 32–39. [PubMed: 11165670]

Gadea G, Sanz-Moreno V, Self A, Godi A, Marshall CJ. DOCK10-Mediated Cdc42 Activation Is Necessary for Amoeboid Invasion of Melanoma Cells. Current Biology. 2008; 18(19):1456–1465. [PubMed: 18835169]

Ganguly A, Yang H, Sharma R, Patel KD, Cabral F. The Role of Microtubules and Their Dynamics in Cell Migration. Journal of Biological Chemistry. 2012

Gass GV, Chernomordik LV. Reversible large-scale deformations in the membranes of electrically-treated cells: electroinduced bleb formation. Biochimica et Biophysica Acta (BBA) - Biomembranes. 1990; 1023(1):1–11.

Guerriero CJ, Weisz OA. N-WASP inhibitor wiskostatin nonselectively perturbs membrane transport by decreasing cellular ATP levels. American Journal of Physiology - Cell Physiology. 2007; 292(4):C1562–C1566. [PubMed: 17092993]

Hummel I, Klappe K, Ercan C, Kok JW. Multidrug Resistance-Related Protein 1 (MRP1) Function and Localization Depend on Cortical Actin. Molecular Pharmacology. 2011; 79(2):229–240. [PubMed: 21045108]

Jordan MA, Toso RJ, Thrower D, Wilson L. Mechanism of mitotic block and inhibition of cell proliferation by taxol at low concentrations. Proceedings of the National Academy of Sciences. 1993; 90(20):9552–9556.

Kardash E, Reichman-Fried M, Maitre J-L, Boldajipour B, Papusheva E, Messerschmidt E-M, Heisenberg C-P, Raz E. A role for Rho GTPases and cell-cell adhesion in single-cell motility in vivo. Nat Cell Biol. 2010; 12(1):47–53. [PubMed: 20010816]

Keely PJ, Westwick JK, Whitehead IP, Der CJ, Parise LV. Cdc42 and Rac1 induce integrin-mediated cell motility and invasiveness through PI(3)K. Nature. 1997; 390(6660):632–636. [PubMed: 9403696]

Kimura K, Ito M, Amano M, Chihara K, Fukata Y, Nakafuku M, Yamamori B, Feng J, Nakano T, Okawa K, Iwamatsu A, Kaibuchi K. Regulation of myosin phosphatase by Rho and Rho-associated kinase (Rho-kinase). Science (New York, NY). 1996; 273(5272):245–248.

Kovács M, Tóth J, Hetényi C, Málnási-Csizmadia A, Sellers JR. Mechanism of Blebbistatin Inhibition of Myosin II. Journal of Biological Chemistry. 2004; 279(34):35557–35563. [PubMed: 15205456]

Lammermann T, Bader BL, Monkley SJ, Worbs T, Wedlich-Soldner R, Hirsch K, Keller M, Forster R, Critchley DR, Fassler R, Sixt M. Rapid leukocyte migration by integrin-independent flowing and squeezing. Nature. 2008; 453(7191):51–55. [PubMed: 18451854]

Lämmermann T, Renkawitz J, Wu X, Hirsch K, Brakebusch C, Sixt M. Cdc42-dependent leading edge coordination is essential for interstitial dendritic cell migration. Blood. 2009; 113(23):5703–5710. [PubMed: 19190242]

Lämmermann T, Sixt M. Mechanical modes of 'amoeboid' cell migration. Current Opinion in Cell Biology. 2009; 21(5):636–644. [PubMed: 19523798]

Leung T, Chen XQ, Manser E, Lim L. The p160 RhoA-binding kinase ROK alpha is a member of a kinase family and is involved in the reorganization of the cytoskeleton. Molecular and Cellular Biology. 1996; 16(10):5313–5327. [PubMed: 8816443]

Limouze J, Straight A, Mitchison T, Sellers J. Specificity of blebbistatin, an inhibitor of myosin II. Journal of Muscle Research and Cell Motility. 2004; 25(4):337–341. [PubMed: 15548862]

Martinet W, Schrijvers DM, Kockx MM. Nucleofection as an efficient nonviral transfection method for human monocytic cells. Biotechnology Letters. 2003; 25(13):1025–1029. [PubMed: 12889809]

Maugis B, Brugues J, Nassoy P, Guillen N, Sens P, Amblard F. Dynamic instability of the intracellular pressure drives bleb-based motility. J Cell Sci. 2010; 123(22):3884–3892. [PubMed: 20980385]

Mills JC, Stone NL, Erhardt J, Pittman RN. Apoptotic Membrane Blebbing Is Regulated by Myosin Light Chain Phosphorylation. The Journal of Cell Biology. 1998; 140(3):627–636. [PubMed: 9456322]

Miron-Mendoza M, Seemann J, Grinnell F. The differential regulation of cell motile activity through matrix stiffness and porosity in three dimensional collagen matrices. Biomaterials. 2010; 31(25):6425–6435. [PubMed: 20537378]

Mitchison TJ, Charras GT, Mahadevan L. Implications of a poroelastic cytoplasm for the dynamics of animal cell shape. Seminars in Cell & Developmental Biology. 2008; 19(3):215–223. [PubMed: 18395478]

Olson M, Sahai E. The actin cytoskeleton in cancer cell motility. Clinical and Experimental Metastasis. 2009; 26(4):273–287. [PubMed: 18498004]

Pakhomov AG, Shevin R, White JA, Kolb JF, Pakhomova ON, Joshi RP, Schoenbach KH. Membrane permeabilization and cell damage by ultrashort electric field shocks. Archives of Biochemistry and Biophysics. 2007; 465(1):109–118. [PubMed: 17555703]

Paluch E, Piel M, Prost J, Bornens M, Sykes C. Cortical Actomyosin Breakage Triggers Shape Oscillations in Cells and Cell Fragments. Biophysical Journal. 2005; 89(1):724–733. [PubMed: 15879479]

Paluch E, Sykes C, Prost J, Bornens M. Dynamic modes of the cortical actomyosin gel during cell locomotion and division. Trends in Cell Biology. 2006; 16(1):5–10. [PubMed: 16325405]

Parri M, Chiarugi P. Rac and Rho GTPases in cancer cell motility control. Cell Commun Signal. 2010; 8:23. [PubMed: 20822528]

Parri M, Taddei ML, Bianchini F, Calorini L, Chiarugi P. EphA2 Reexpression Prompts Invasion of Melanoma Cells Shifting from Mesenchymal to Amoeboid-like Motility Style. Cancer Research. 2009; 69(5):2072–2081. [PubMed: 19244130]

Paul BZS, Daniel JL, Kunapuli SP. Platelet Shape Change Is Mediated by both Calcium-dependent and -independent Signaling Pathways: Role Of p160 Rho-Associated Coiled-Coil-Containing Protein Kinase In Platelet Shape Change. Journal of Biological Chemistry. 1999; 274(40):28293–28300. [PubMed: 10497186]

Peterson JR, Bickford LC, Morgan D, Kim AS, Ouerfelli O, Kirschner MW, Rosen MK. Chemical inhibition of N-WASP by stabilization of a native autoinhibited conformation. Nat Struct Mol Biol. 2004; 11(8):747–755. [PubMed: 15235593]

Petrie RJ, Gavara N, Chadwick RS, Yamada KM. Nonpolarized signaling reveals two distinct modes of 3D cell migration. The Journal of Cell Biology. 2012; 197(3):439–455. [PubMed: 22547408]

Pollard TD, Borisy GG. Cellular Motility Driven by Assembly and Disassembly of Actin Filaments. Cell. 2003; 112(4):453–465. [PubMed: 12600310]

Raftopoulou M, Hall A. Cell migration: Rho GTPases lead the way. Developmental Biology. 2004; 265(1):23–32. [PubMed: 14697350]

Rassokhin M, Pakhomov A. Electric Field Exposure Triggers and Guides Formation of Pseudopod-Like Blebs in U937 Monocytes. Journal of Membrane Biology. 2012; 245(9):521–529. [PubMed: 22638933]

Renkawitz J, Sixt M. Mechanisms of force generation and force transmission during interstitial leukocyte migration. EMBO Rep. 2010; 11(10):744–750. [PubMed: 20865016]

Ridley Anne J. Life at the Leading Edge. Cell. 2011; 145(7):1012–1022. [PubMed: 21703446]

Ridley AJ, Paterson HF, Johnston CL, Diekmann D, Hall A. The small GTP-binding protein rac regulates growth factor-induced membrane ruffling. Cell. 1992; 70(3):401–410. [PubMed: 1643658]

Ridley AJ, Schwartz MA, Burridge K, Firtel RA, Ginsberg MH, Borisy G, Parsons JT, Horwitz AR. Cell Migration: Integrating Signals from Front to Back. Science. 2003; 302(5651):1704–1709. [PubMed: 14657486]

Rohatgi R, Ma L, Miki H, Lopez M, Kirchhausen T, Takenawa T, Kirschner MW. The Interaction between N-WASP and the Arp2/3 Complex Links Cdc42-Dependent Signals to Actin Assembly. Cell. 1999; 97(2):221–231. [PubMed: 10219243]

Rottner K, Hall A, Small JV. Interplay between Rac and Rho in the control of substrate contact dynamics. Current Biology. 1999; 9(12):S640–S641.

Sahai E, Marshall CJ. Differing modes of tumour cell invasion have distinct requirements for Rho/ROCK signalling and extracellular proteolysis. Nat Cell Biol. 2003; 5(8):711–719. [PubMed: 12844144]

Salbreux G, Charras G, Paluch E. Actin cortex mechanics and cellular morphogenesis. Trends in Cell Biology. 2012; 22(10):536–545. [PubMed: 22871642]

Sanz-Moreno V. Tumour Invasion: A New Twist on Rac-Driven Mesenchymal Migration. Current Biology. 2012; 22(11):R449–R451. [PubMed: 22677287]

Sanz-Moreno V, Gadea G, Ahn J, Paterson H, Marra P, Pinner S, Sahai E, Marshall CJ. Rac Activation and Inactivation Control Plasticity of Tumor Cell Movement. Cell. 2008; 135(3):510–523. [PubMed: 18984162]

Schoenbach KH, Hargrave B, Joshi RP, Kolb JF, Nuccitelli R, Osgood C, Pakhomov A, Stacey M, Swanson RJ, White JA, Shu X, Jue Z, Beebe SJ, Blackmore PF, Buescher ES. Bioelectric Effects of Intense Nanosecond Pulses. Dielectrics and Electrical Insulation, IEEE Transactions on. 2007; 14(5):1088–1109.

Semenov I, Xiao S, Pakhomov AG. Primary pathways of intracellular Ca(2+) mobilization by nanosecond pulsed electric field. Biochimica et Biophysica Acta (BBA) - Biomembranes. 2012; (0)

Steffen A, Rottner K, Ehinger J, Innocenti M, Scita G, Wehland J, Stradal TEB. Sra-1 and Nap1 link Rac to actin assembly driving lamellipodia formation. EMBO J. 2004; 23(4):749–759. [PubMed: 14765121]

Taddei ML, Parri M, Angelucci A, Bianchini F, Marconi C, Giannoni E, Raugei G, Bologna M, Calorini L, Chiarugi P. EphA2 Induces Metastatic Growth Regulating Amoeboid Motility and Clonogenic Potential in Prostate Carcinoma Cells. Molecular Cancer Research. 2011; 9(2):149–160. [PubMed: 21205836]

Takesono A, Heasman SJ, Wojciak-Stothard B, Garg R, Ridley AJ. Microtubules Regulate Migratory Polarity through Rho/ROCK Signaling in T Cells. PLoS ONE. 2010; 5(1):e8774. [PubMed: 20098744]

Tan JL, Ravid S, Spudich JA. Control of Nonmuscle Myosins by Phosphorylation. Annual Review of Biochemistry. 1992; 61(1):721–759.

Tekle E, Wolfe MD, Oubrahim H, Chock PB. Phagocytic clearance of electric field induced 'apoptosis-mimetic' cells. Biochemical and Biophysical Research Communications. 2008; 376(2): 256–260. [PubMed: 18771656]

Tsong TY. Electroporation of cell membranes. Biophys J. 1991; 60(2):297–306. [PubMed: 1912274]

Vega FM, Fruhwirth G, Ng T, Ridley AJ. RhoA and RhoC have distinct roles in migration and invasion by acting through different targets. The Journal of Cell Biology. 2011; 193(4):655–665. [PubMed: 21576392]

Vicente-Manzanares M, Ma X, Adelstein RS, Horwitz AR. Non-muscle myosin II takes centre stage in cell adhesion and migration. Nat Rev Mol Cell Biol. 2009; 10(11):778–790. [PubMed: 19851336]

Vicente-Manzanares M, Webb DJ, Horwitz AR. Cell migration at a glance. Journal of Cell Science. 2005; 118(21):4917–4919. [PubMed: 16254237]

White JA, Blackmore PF, Schoenbach KH, Beebe SJ. Stimulation of Capacitative Calcium Entry in HL-60 Cells by Nanosecond Pulsed Electric Fields. Journal of Biological Chemistry. 2004; 279(22):22964–22972. [PubMed: 15026420]

Wolf K, Mazo I, Leung H, Engelke K, von Andrian UH, Deryugina EI, Strongin AY, Bröcker E-B, Friedl P. Compensation mechanism in tumor cell migration. The Journal of Cell Biology. 2003a; 160(2):267–277. [PubMed: 12527751]

Wolf K, Müller R, Borgmann S, Bröcker E-B, Friedl P. Amoeboid shape change and contact guidance: T-lymphocyte crawling through fibrillar collagen is independent of matrix remodeling by MMPs and other proteases. Blood. 2003b; 102(9):3262–3269. [PubMed: 12855577]

Yam PT, Wilson CA, Ji L, Hebert B, Barnhart EL, Dye NA, Wiseman PW, Danuser G, Theriot JA. Actin–myosin network reorganization breaks symmetry at the cell rear to spontaneously initiate polarized cell motility. The Journal of Cell Biology. 2007; 178(7):1207–1221. [PubMed: 17893245]

Yoshida K, Soldati T. Dissection of amoeboid movement into two mechanically distinct modes. Journal of Cell Science. 2006; 119(18):3833–3844. [PubMed: 16926192]
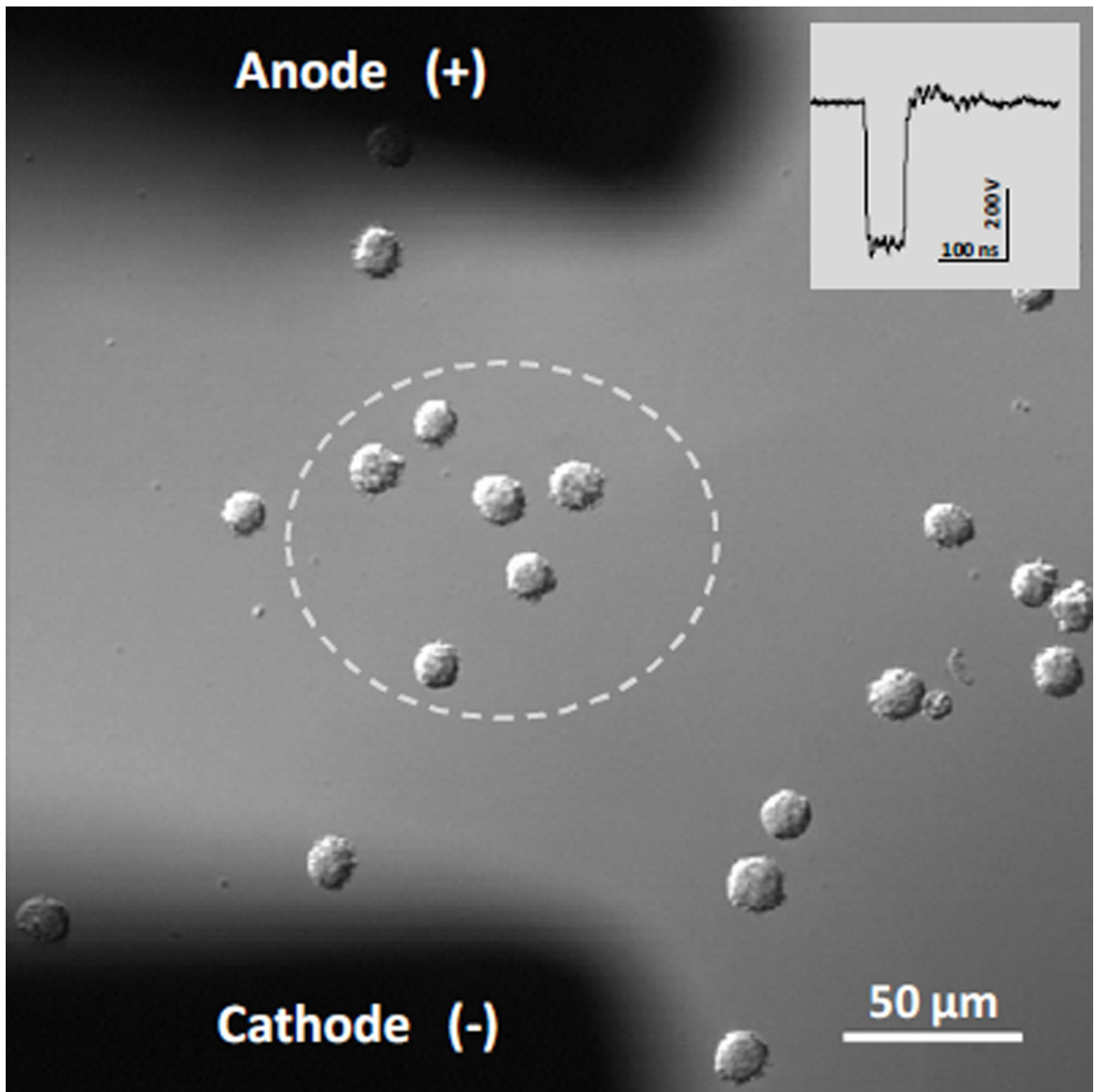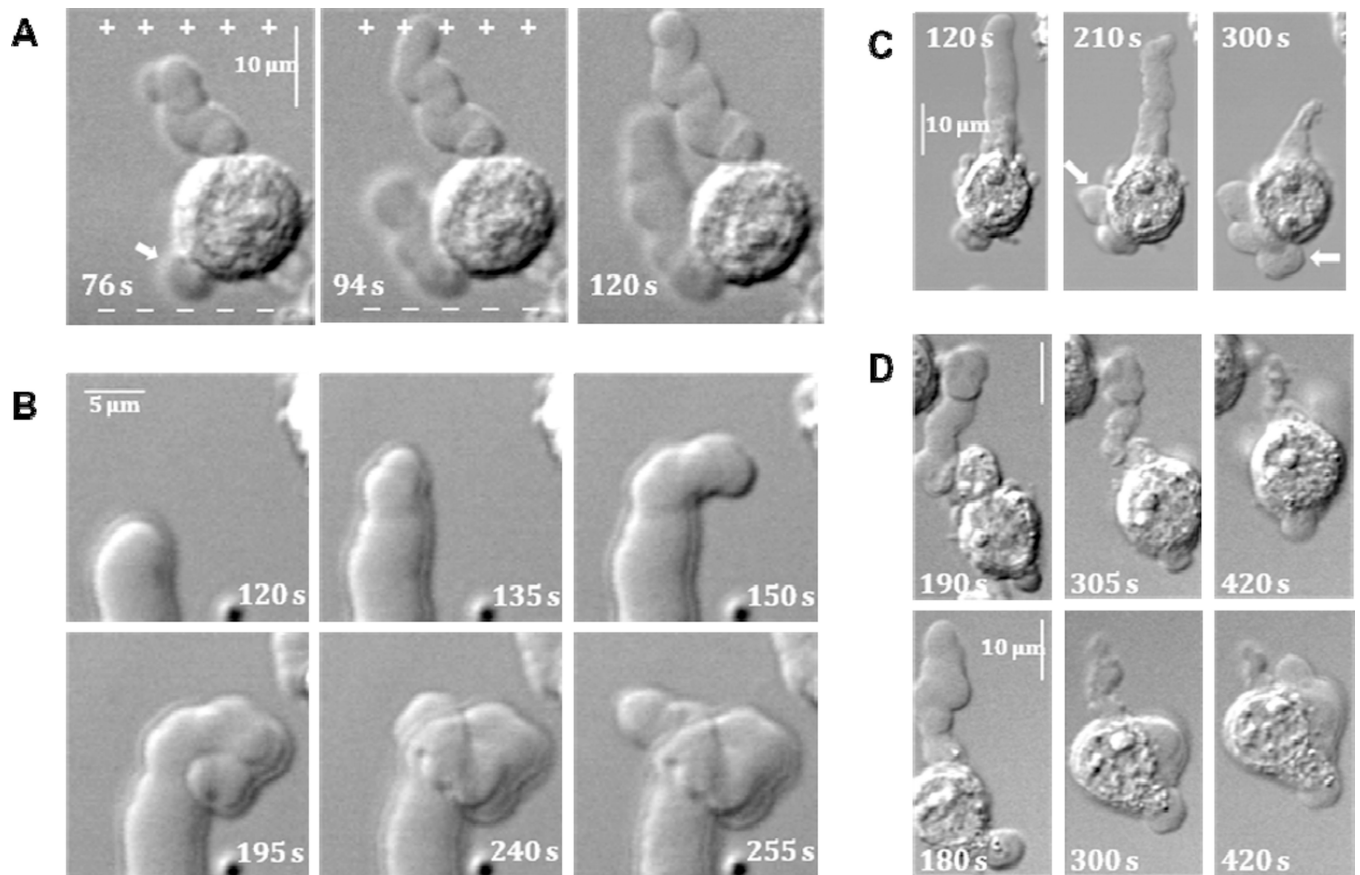
Figure 1.
NsPEF exposure of U937 cells on a cover slip. The electric field is practically uniform (+/− 15%) within the area bordered by the dashed line. The inset shows the waveform of a single 60 ns electric pulse. For a 400-V pulse (shown), the E-field within the dashed area is about 12 kV/cm. Electrodes layout is identical in all subsequent figures.
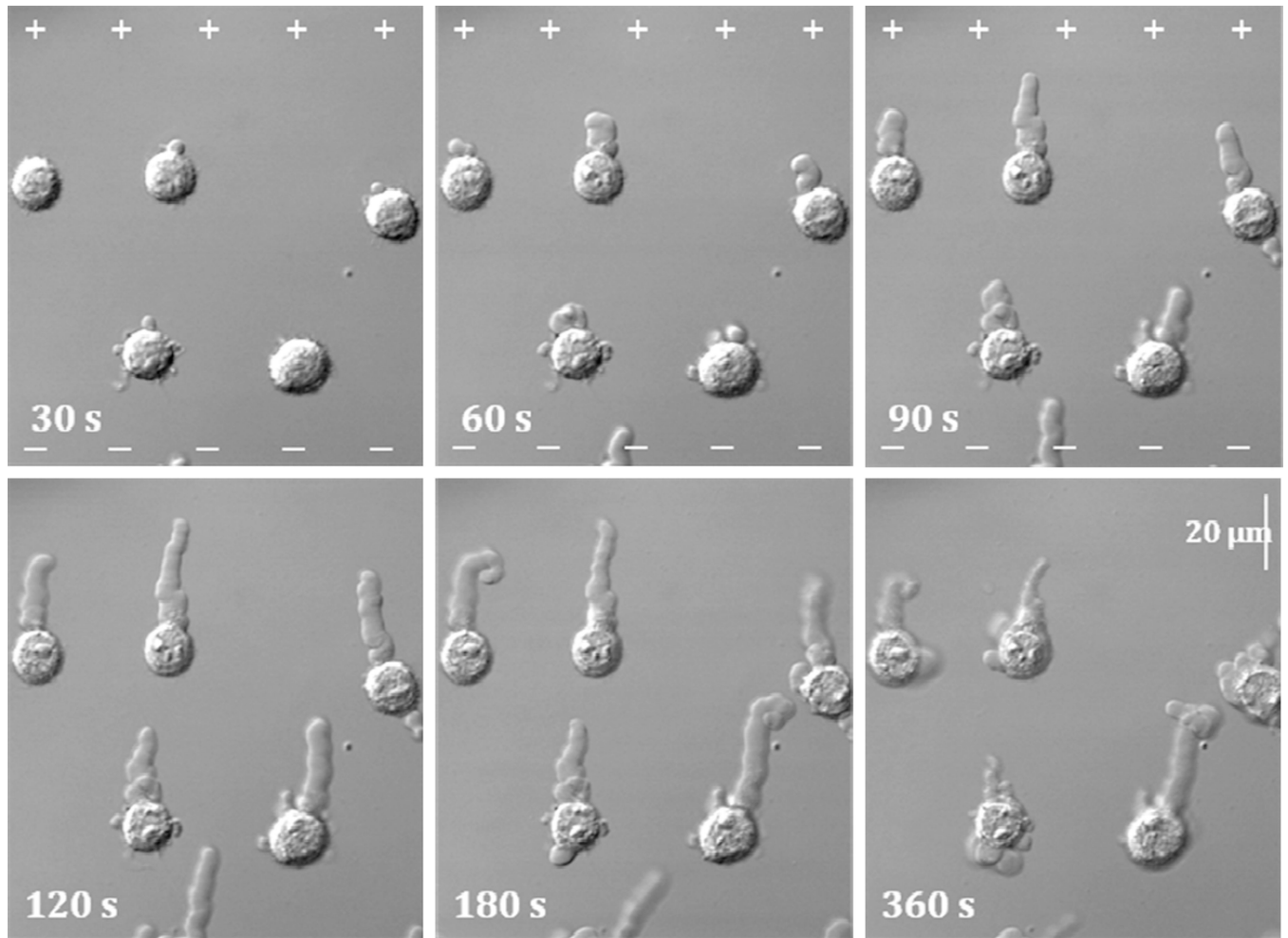
Figure 2.
Nanosecond pulsed electric field (nsPEF) exposure triggers and guides extension of PLBs.
U937 cells are shown at selected timepoints during and after nsPEF exposure (hereinafter 0
to 119 s). PLBs nucleate at 30 s and extend toward anode (+) throughout the exposure.
Hereinafter, the anode (+) and cathode (−) directions are shown only on those images that
were taken during nsPEF treatment. After the end of pulse train (120 s), PLBs may keep
growing for a short while but in arbitrary direction (180 s), then retract (360 s).

Figure 3.
Distinctive features of PLB formation and lifecycle. For all panels, nsPEF exposure lasts from 0 s to 119 s, and the position of electrodes with respect to cells is the same as in Figs. 1 and 2.

A: nsPEF guides PLB growth towards anode even if PLB starts elsewhere on the cell body. In the cell shown, a bleb that nucleated on the left side of the cell body (arrow, 76 s) later turns and grows towards anode (+).

B : Undirected PLB growth after the end of nsPEF exposure. Sequential images illustrate the loss of directionality of PLB in one of the cells from Fig. 2.

C : The volume of liquid extruded from PLB during its shrinkage following nsPEF exposure is accommodated in secondary blebs (arrows).

D: Examples of cell translocation by PLB contraction. Upper and lower row show two individual cells from different experiments.
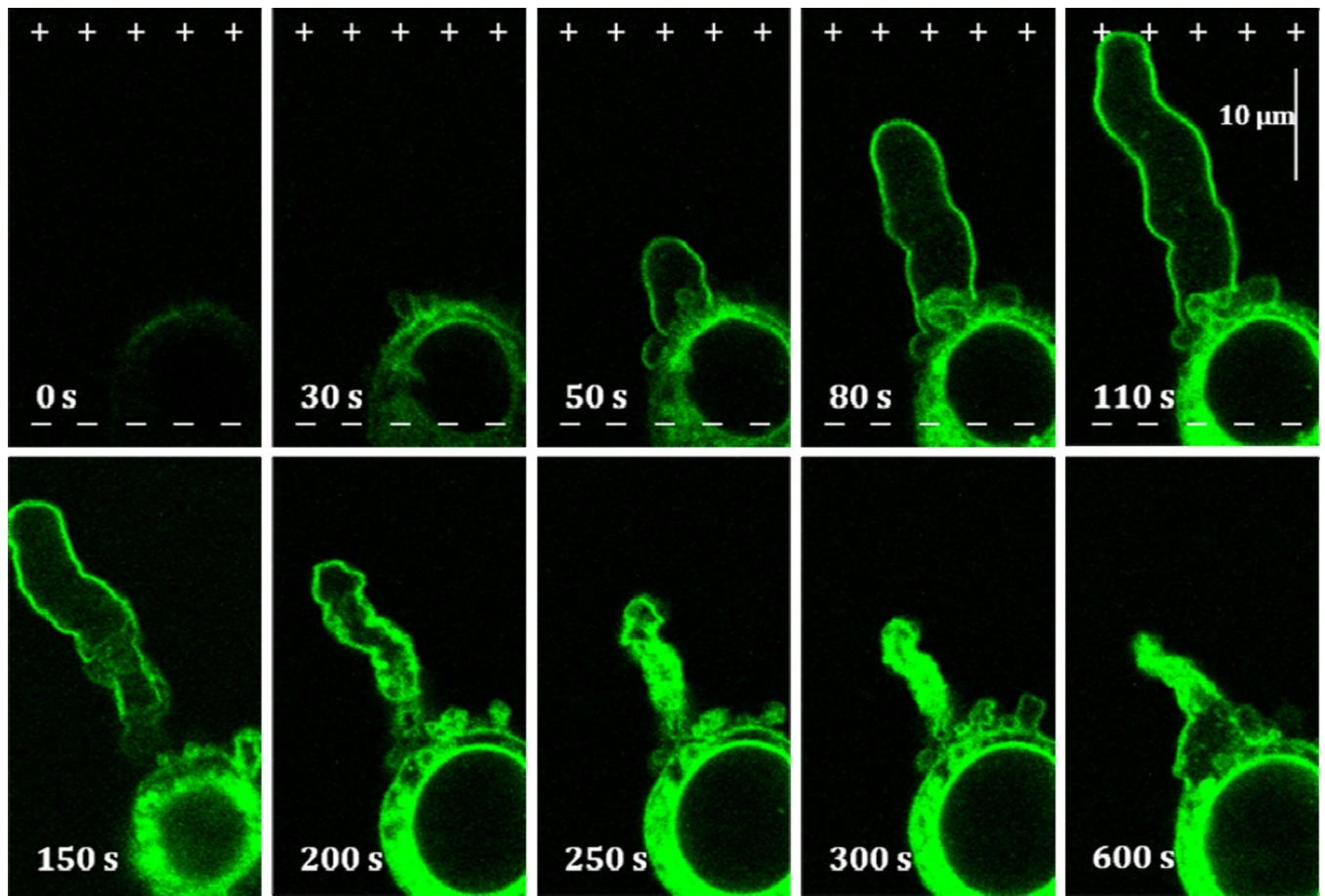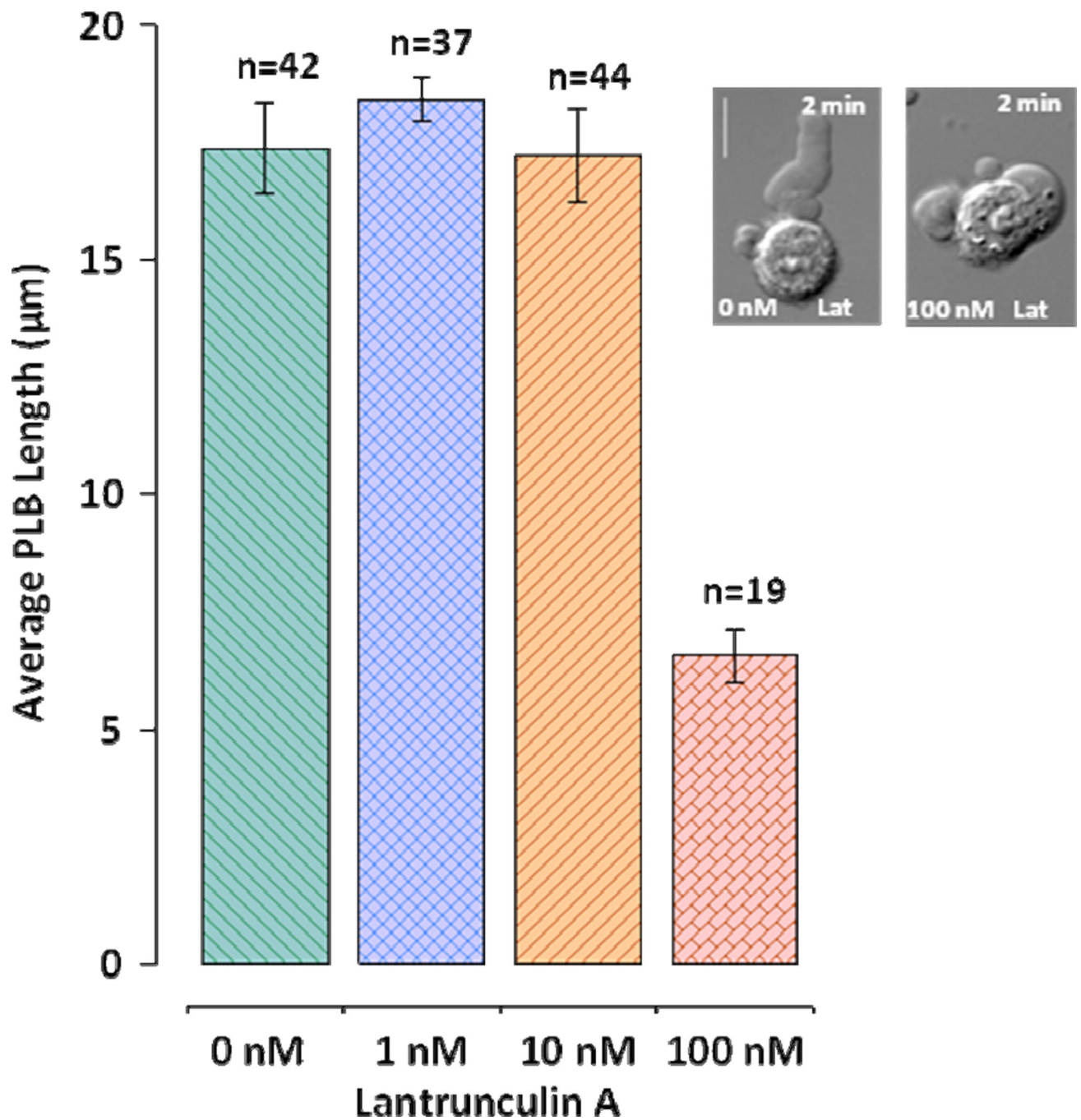
Figure 4.
Formation and contraction of actin cortex in PLB during extension and retraction. Oregon-Green® 488-phalloidin conjugate enters electropermeabilized cell on the anodic pole (0–30 s). A layer of actin cortex that forms during PLB extension (50–110 s) thickens and crumples during contraction (150–600 s). See text and Figs. 1 and 2 for more detail.
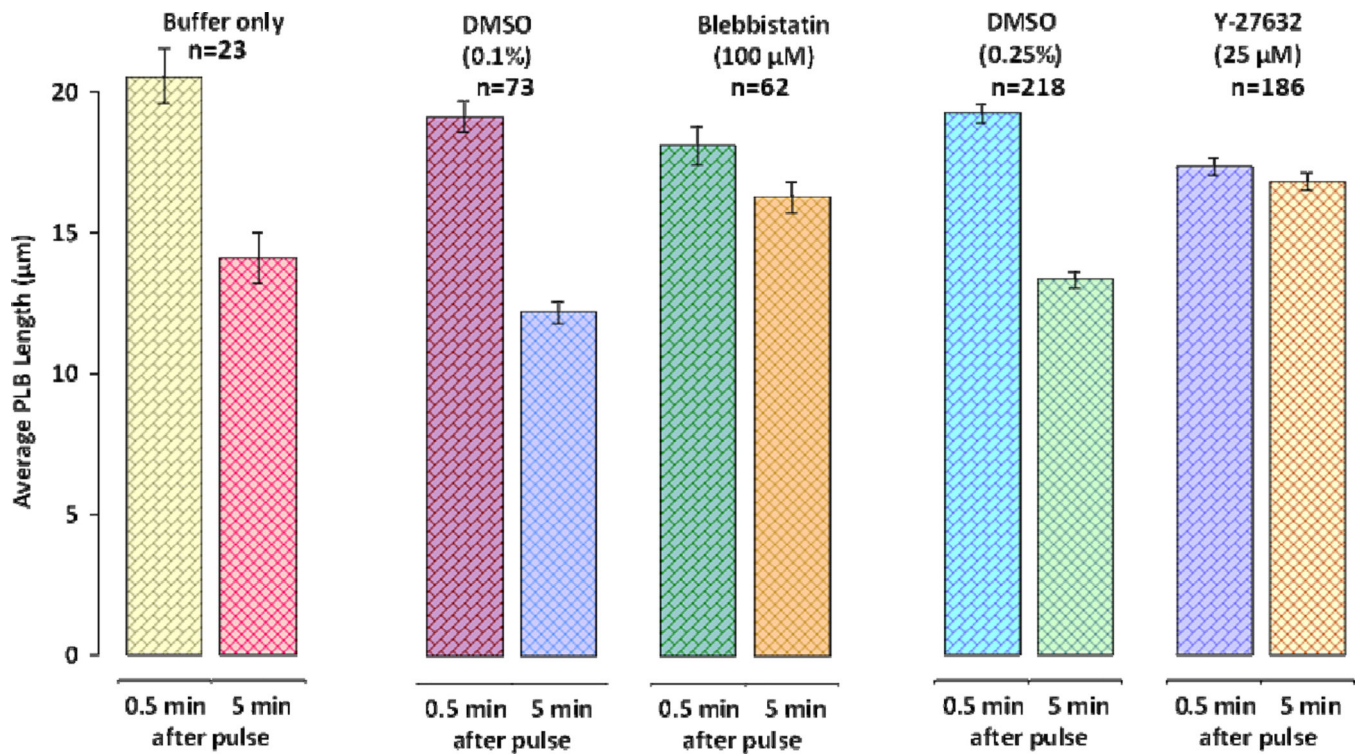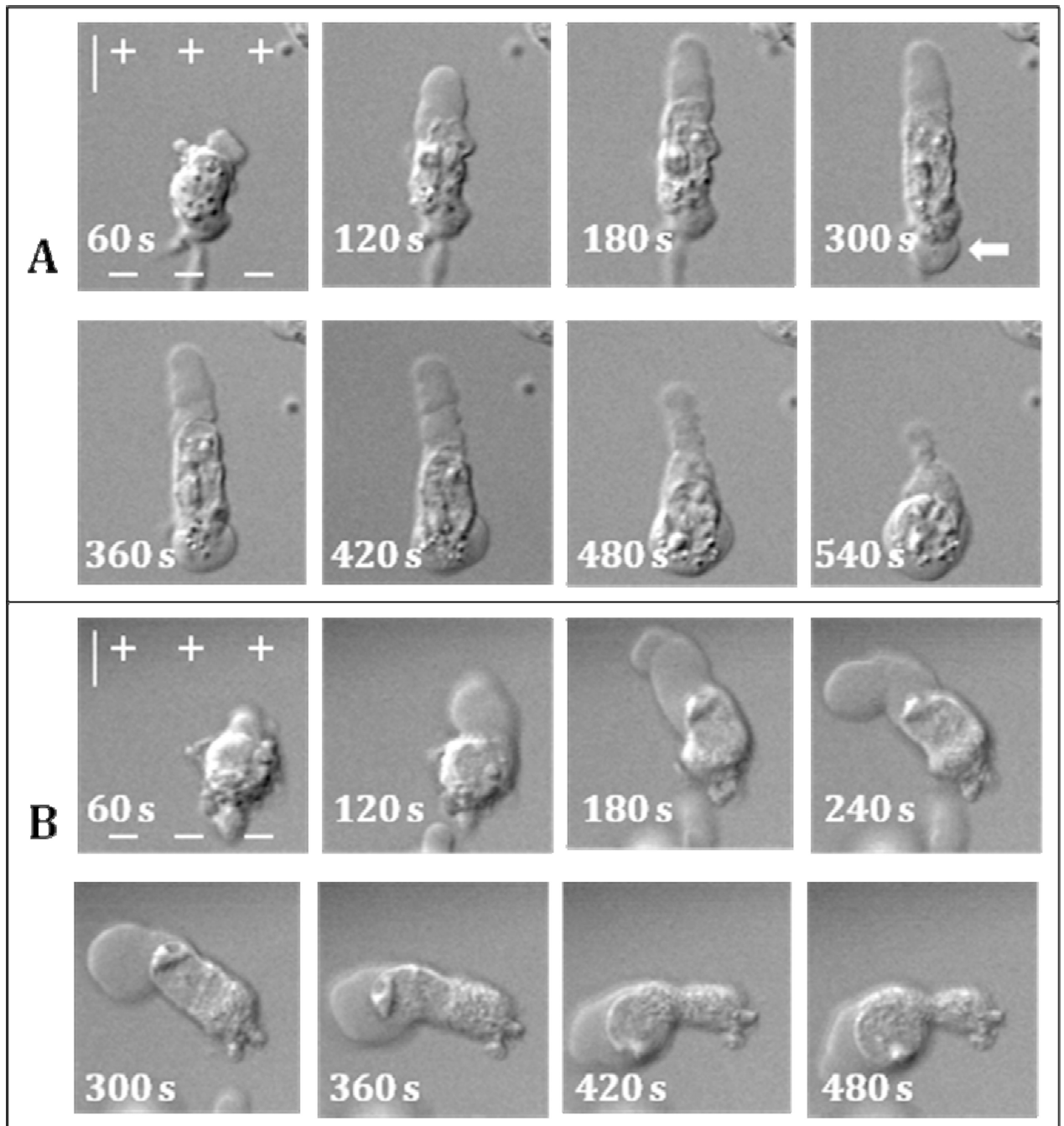
Figure 5.
Inhibition of contractility prevents PLB retraction but has no effect on extension. The peak extension of PLBs was measured at 0.5 min and peak retraction at 5 min after nsPEF exposure. Note that these timepoints correspond to 150 s and 420 s of recordings, respectively. The data are presented as mean +/− S.E. for the following groups: control (buffer only), vehicle controls (DMSO 0.1 and 0.25%), blebbistatin in 0.1% DMSO and Y-27632 in 0.25% DMSO. The inhibition of PLB contraction by blebbistatin and Y-27632 is statistically significant at p<0.01 (Student's t-test) as compared to respective vehicle controls.
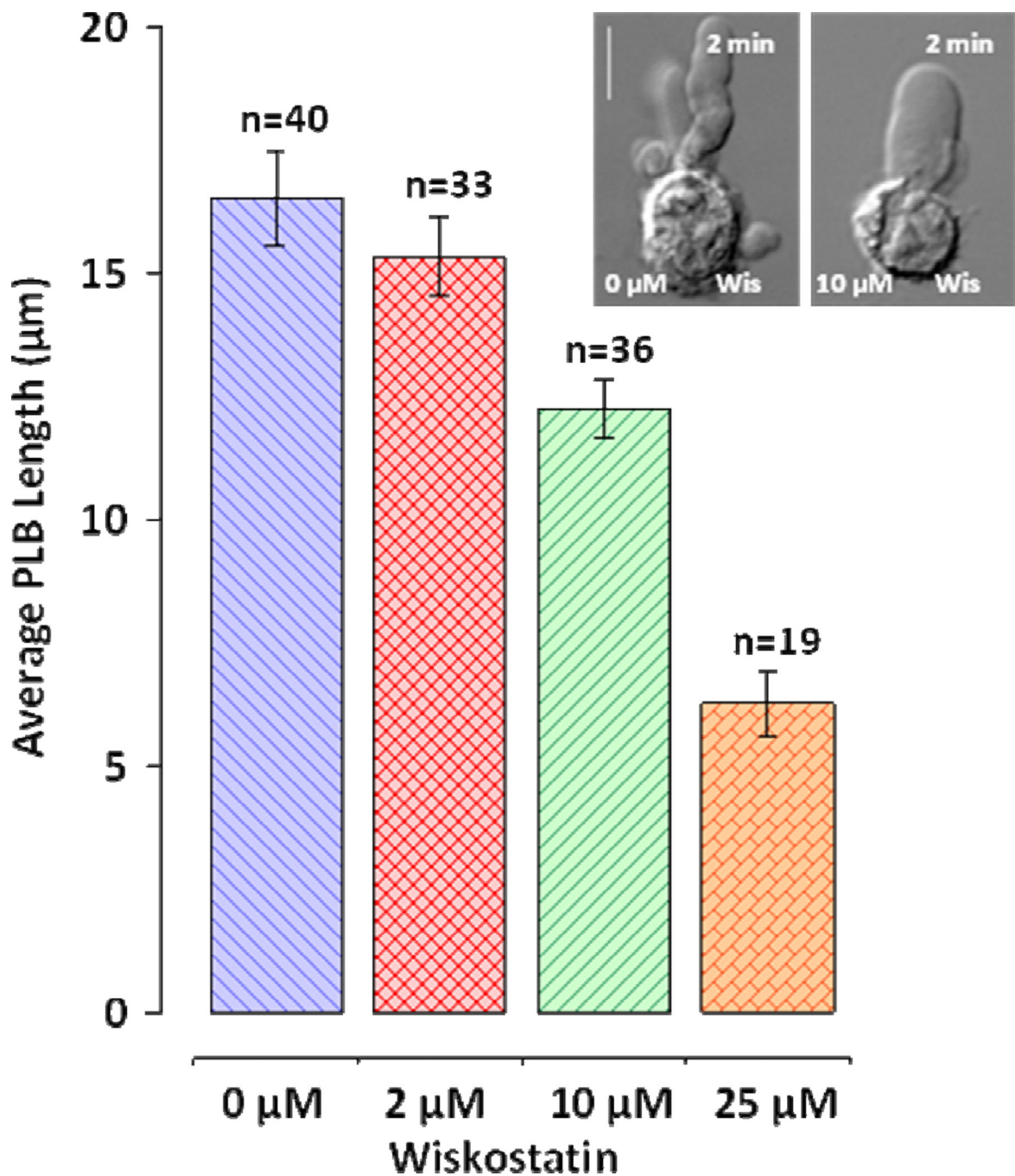
Figure 6.
Inhibition of actin polymerization by latrunculin A prevents PLB growth but not nucleation of blebs. PLB length (mean +/− S.E.) was measured at its maximum immediately after the nsPEF treatment. Only inhibition by 100 nM latrunculin A is significant (p<0.01, Student's t-test) as compared to control. Cells were placed in the drug-containing buffer immediately prior to nsPEF treatment. The scale bar is 10 μm. The inset shows typical blebs formed in the control buffer and in the presence of 100 nM latrunculin A. See text for more detail.

Figure 7.
Destruction of microtubules increases mobility and deformation of nuclei during PLB extension and retraction. NsPEF exposure is from 0 s to 119 s. A and B: two individual cells that show different behavior of cell nucleus after nocodazole treatment. In A, the nucleus gets pulled into PLB but then migrates back and into the secondary bleb on the cathodic cell pole (arrow). In B, nucleus squeezes through PLB neck and enters bleb lumen. The scale is 10 μm. See text and Figs. 1 and 2 for more detail.

Figure 8.
Inhibition of WASP by wiskostatin inhibits PLB growth. Peak PLB length (mean +/− S.E.) was measured immediately after nsPEF treatment. Cells were placed in the drug-containing buffer immediately prior to nsPEF treatment. Inhibition by 10 μM and 25 μM wiskostatin is significant at p<0.01 (Student's t-test) as compared to control. The scale bar is 10 μm. The inset shows typical blebs formed in the control buffer and in the presence of 10 μM wiskostatin. Note concurrent thickening and shortening of PLB. See text for more detail.